

Intermolecular Interactions in Crystals of the Photosensitive Coordination Compounds of Zinc(II)

A. V. Vologzhanina^{a, *}, E. N. Zorina-Tikhonova^b, A. S. Chistyakov^b, A. A. Sidorov^b,
A. A. Korlyukov^a, and I. L. Eremenko^{a, b}

^aNesmeyanov Institute of Organoelement Compounds, Russian Academy of Sciences, Moscow, 119991 Russia

^bKurnakov Institute of General and Inorganic Chemistry, Russian Academy of Sciences,
Moscow, 119991 Russia

*e-mail: vologzhanina@mail.ru

Received December 11, 2017

Abstract—The distribution of the electron density function in crystals of $\{[\text{ZnBpe}(\text{Me}_2\text{Mal})]\cdot\text{H}_2\text{O}\}_n$ (I) and $[\text{Zn}(\text{H}_2\text{O})_4\text{Bpe}_2](\text{HEt}_2\text{Mal})_2$ (II) is obtained by the periodic DFT calculations. Under UV irradiation, compounds I and II transform into $[\text{Zn}(\text{Bpe})(\text{Me}_2\text{Mal})]\cdot[\text{Zn}_2(\text{Tpcb})(\text{Me}_2\text{Mal})_2]\cdot\text{H}_2\text{O}$ and $\{[\text{Zn}(\text{H}_2\text{O})_4(\text{Bpe})]_{0.15}[\text{Zn}(\text{H}_2\text{O})_4(\text{Tpcb})]_{0.85}(\text{HEt}_2\text{mMal})_4\}$ (Bpe is 1,2-bis(4-pyridine)ethylene, Tpcb is 1,2,3,4-tetrakis(4-pyridine)cyclobutane, $\text{H}_2\text{Me}_2\text{Mal}$ is dimethylmalonic acid, and $\text{H}_2\text{Et}_2\text{Mal}$ is diethylmalonic acid), respectively. An analysis of intermolecular contacts using Bader's “Atoms-in-Molecules” theory shows the bonding route and bond critical point between the carbon atoms of the adjacent 1,2-bis(4-pyridine)ethylene molecules. It is established that the common surface of the Voronoi–Dirichlet molecular polyhedra between the photosensitive fragments can serve as a criterion for the possible participation of the molecules in solid-phase photoinduced reactions.

Keywords: zinc(II) complexes, Voronoi–Dirichlet polyhedra, periodic DFT calculations

DOI: 10.1134/S1070328418100111

INTRODUCTION

Solid-phase reactions represent one of the methods for the synthesis of organic and coordination compounds, the uniqueness of which is the controlled arrangement of the reactants in the initial step [1–3]. Unlike reactions in solutions, the latter does not always take place and proceeds to the direction of only one of several possible reaction products if occurs [4, 5]. Moreover, this method allows one to obtain such unique compounds as polyanion-based 3D periodic coordination polymers and hypercrosslinked coordination polymers [6–9]. The possibility to study the structure of the compound before, during, and after the reaction provides a unique opportunity to characterize intermediates and to establish the mechanism and kinetics of the reaction [10–14]. Unfortunately, active molecules cannot always be arranged in positions that allow one to carry out the reaction, especially in coordination compounds. Therefore, the search for methods that would extend the range of possible reactions is of doubtless interest. For example, it is well known that photochemical [2+2] addition occurs in the solid state if the d distance between the $\text{C}=\text{C}$ bonds does not exceed 4.2 Å, and the coplanar and parallel arrangement of these fragments ($\theta = 0^\circ$, $\theta_1 = 90^\circ$, $\theta_2 = 90^\circ$) is also desirable [15]. The

arrangement of the ethylene fragments relative to each other and the geometric parameters characterizing this arrangement are schematically shown below.



Therefore, the search in the Cambridge Structural Database for all compounds characterized by the “successful” arrangement of double bonds could facilitate searching for precursors for solid-phase reactions. However, even in this case, the reaction is not warranted to occur, because a similar geometric approach ignores the shielding of reaction groups by other atoms and groups of atoms and electronic effects of substituents [16].

It is reasonable to assume that if a bond critical point corresponding to the $\pi\cdots\pi$ interaction between the reactive carbon atoms and the corresponding bonding route exist, the latter would serve as a channel via which the electron density is redistributed in the case of photoinitiation. In other words, the study of the function of the electron density distribution in a crystal of the compound containing photosensitive fragments makes it possible to predict more reliably

the possibility of the reaction to occur. This method is restricted by time expenses and, hence, more approximate methods of crystal chemical analysis of intermolecular bonds are also interesting.

In this work, we check the ability of Bader's "Atoms-in-Molecules" (AM) theory [17] and the stereoatomic model of the structure of matter [18] (which showed a good qualitative correspondence for the description of weak intermolecular bonds with the AM theory) to predict the possibility of photoinduced [2+2] addition to occur for some coordination compounds of zinc with 1,2-bis(4-pyridine)ethylene (Bpe) and substituted malonic acids for which these reactions have recently been discovered [19].

EXPERIMENTAL

Periodic DFT calculations were performed in the Vienna Ab-initio Simulation Package (VASP) 5.4.1 program package [20–22]. The experimental coordinates of atoms were used for structure optimization, but the initial structural models were measured in such a way that disordering caused by symmetry elements would be removed. Valence electrons were described by a set of planar waves (the maximum kinetic energy was 800 eV), whereas the electrons of the atomic frameworks were refined by the PAW (projected augmented waves) type potentials. The exchange and correlation contributions to the total energy were calculated using the PBE functional. A D3 correction was used to apply the dispersion contribution to the total energy [23]. After optimization, the forces on the atoms were lower than 0.01 eV \AA^{-1} . The electron density function for topological analysis in terms of the AM theory was specially calculated using the optimized coordinates of atoms and an exacter network of the Fourier transform. The topological analysis of the electron density was performed using the CRITIC2 program [24].

Intermolecular contacts were analyzed in terms of the stereoatomic model of the structure of matter using the ToposPro program package [25].

RESULTS AND DISCUSSION

The syntheses of $\{[\text{ZnBpe}(\text{Me}_2\text{Mal})] \cdot \text{H}_2\text{O}\}_n$ (**I**), $[\text{Zn}(\text{H}_2\text{O})_4\text{Bpe}_2](\text{HET}_2\text{Mal})_2$ (**II**), and $[\text{ZnBpe}(\text{Et}_2\text{Mal})] \cdot 0.25\text{Bpe}$ (**III**) were described [19]. The [2+2] addition reaction was confirmed to occur for these compounds by single crystal and powder X-ray diffraction analyses and ^1H NMR. The [2+2] addition of compounds **I**, **II**, and **III** proceeds via the types $3\text{D} \rightarrow 3\text{D}$ (formation of a "hypercrosslinked" coordination polymer with a new topology), $0\text{D} \rightarrow 1\text{D}$ (closure of the island complexes to form a chain), and $3\text{D} \rightarrow 3\text{D}$ (addition of the uncoordinated Bpe molecule to the coordination polymer), respectively. The mutual arrangement of the Bpe molecules in crystals

of compounds **I** and **II** demonstrates two different cases of their mutual orientation affecting the reaction product (Fig. 1). The d distance (between the centers of the double bonds) in a molecule of compound **I** is 4.14 \AA , and the θ , θ_1 , and θ_2 angles are 28° , 77° , and 80° , which is rather far from optimum values of 0° , 90° , and 90° , respectively. The corresponding values for crystals of compound **II** are 3.74 \AA , 0° , 71° , and 89° , which is much closer to the optimum parameters and can be a reason for the almost complete conversion of 1,2-bis(4-pyridine)ethylene molecules to 1,2,3,4-tetrakis(4-pyridine)cyclobutane (Tpcb), unlike compounds **I** and **III**. Also note that the initial arrangement of the hydrogen atoms at the double bond above each other in compounds **II** and **III** and above the heterocycles in compound **I** results in the formation of different Tpcb isomers: *rctt*, *rcrt*, and *rctc*, respectively. In the case of compound **III**, both periodic quantum-chemical calculations and analysis in the framework of the stereoatomic model are difficult because of the high symmetry of the crystal, since both the Bpe molecules and anions are symmetrically disordered. Therefore, the further analysis was carried out only for compounds **I** and **II**.

In terms of the stereoatomic model of the structure of matter, the Voronoi–Dirichlet polyhedron formed by the planes passing through the middles of the $\text{A}–\text{Y}_i$ contacts (perpendicularly to them) serves as an image of atom A surrounded by atoms Y . In turn, the range of action of the molecule is restricted by the Voronoi–Dirichlet molecular polyhedron consisting of the Voronoi–Dirichlet polyhedra of all atoms of the molecule [26–28]. The Voronoi–Dirichlet molecular polyhedra of the 1,2-bis(4-pyridine)ethylene molecules in the structures of compounds **I** and **II** are shown in Figs. 2a and 3a. In the framework of this model, the criterion of an intermolecular bond is the presence of a common molecular surface are between two molecules [29–31], and the total surface area is proportional to strength of this interaction. Advantages of this model are the possibility of the automatic calculation of descriptors of atoms, molecules, and various types of intermolecular interactions, the possibility of taking into account screening of an atom by other atoms and groups of atoms, and the complete division of the crystalline space into ranges of action of molecules. However, the simplicity of the model results in a fairly approximate (semiquantitative) description of intermolecular interactions. For example, since electronegativities of atoms and the shift of interatomic surface to a less electronegative atom are ignored, this model overestimates the role of weak hydrogen bonds in the stabilization of the crystal lattice [29, 30]. Therefore, it seems reasonable to evaluate the strength of $\pi \cdots \pi$ contacts as a sum of the surface per C/C, C/H, and H/H contacts.

The common intermolecular surface for the adjacent Bpe molecules in the structures of compounds **I**

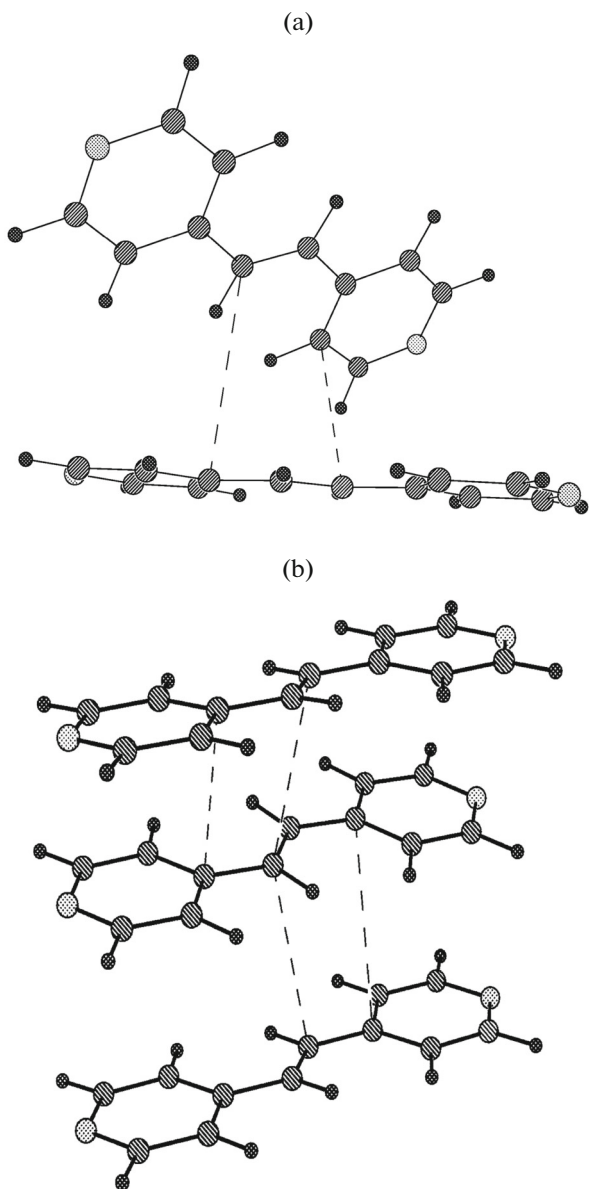


Fig. 1. Mutual arrangement of the Bpe molecules in crystals of compounds (a) **I** and (b) **II**. Intermolecular bonds for which the bond critical points (3, -1) were confirmed by the AM theory are shown by dash.

and **II** is exemplified in Figs. 2b and 3b. For compound **I**, the common surface area of contacts is 3.9 \AA^2 (only 1.6% of the overall molecular surface), where 0.7, 2.8, and 0.4 \AA^2 fall onto the fraction of the C/C, C/H, and H/H interactions, respectively. For compound **II**, the surface area of contacts is higher (5.9 \AA^2 , 2.5% of the overall molecular surface) and is summated of the C/C and C/H interactions (0.9 and 5.0 \AA^2). Note that the [2+2] addition reaction in complex **I** is two-step, where some water molecules are removed in air (the reaction does not occur in a nitrogen flow) in the first step, probably, due to an addi-

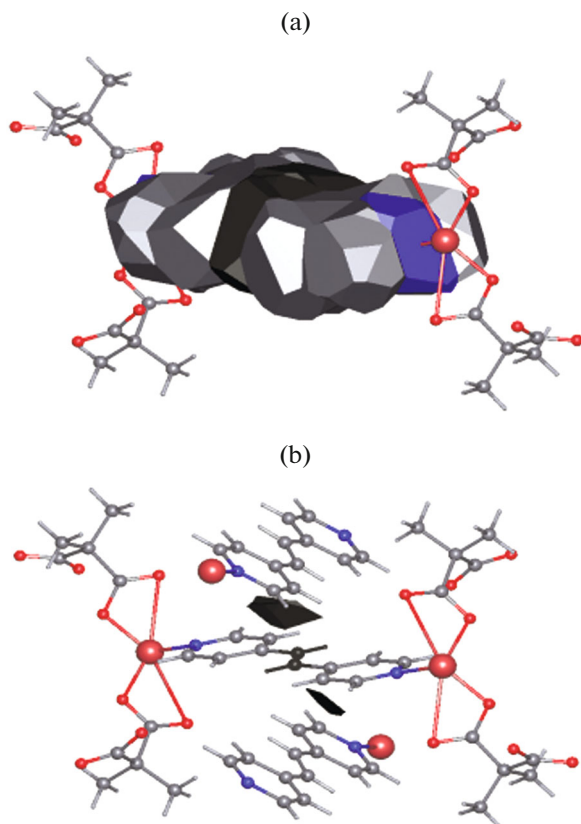
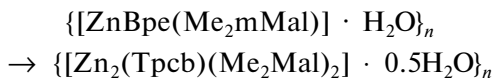


Fig. 2. (a) Voronoi–Dirichlet molecular polyhedron of the Bpe molecule in the structure of compound **I** and (b) its surface area common for the ethylene fragments of two Bpe molecules. Ethylene fragments are shown by black.

tional heating of the crystals from the UV source, and only then two ethylene fragments interact. The removal of some water molecules can lead to an increase in the overall surface area of the molecular surface corresponding to the enhancement of intermolecular contacts. Since the conversion is incomplete in both steps, the final yield of the reaction



is 50% according to the X-ray diffraction data, i.e., the reaction product is $\{[\text{Zn}(\text{Bpe})(\text{Me}_2\text{Mal})]_2 \cdot [\text{Zn}_2(\text{Tpcb})(\text{Me}_2\text{Mal})_2] \cdot \text{H}_2\text{O}\}_n$. The influence of an uncoordinated water molecule on the regularities of the reaction is presently studied additionally.

The topological analysis of the experimental function $\rho(\mathbf{r})$ in crystals of compounds **I** and **II** allowed us to reveal all expected critical points (3, -1) in the regions of coordination and covalent bonds. After geometry optimization, the Zn–N and Zn–O bonds are elongated by 0.01 and 0.02 \AA compared to the experimental bond lengths. According to the calculation results, in compound **I** the zinc atom has the coordination number 4, since the bond critical points

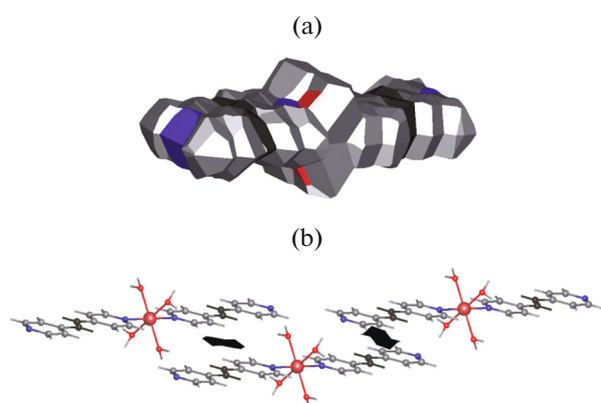


Fig. 3. (a) Voronoi-Dirichlet molecular polyhedron of the Bpe molecule in the structure of compound **II** and (b) its surface area common for the ethylene fragments of two Bpe molecules. Ethylene fragments are shown by black.

corresponding to the interactions of the metal atom and carboxylic groups were observed only for one (nearest) of two oxygen atoms. In compound **II**, as should be expected for the metal atom in the octahedral environment, six critical points involving the zinc(II) atom were found. The bonds involving zinc atoms are characterized by positive $\nabla^2\rho(\mathbf{r})$ values and the negative local density of the electron energy $h_e(\mathbf{r})$ (Table 1), which makes it possible to assign them to interactions of an intermediate type. The results of analysis of the intermolecular interactions involving the carbon atoms of the ethylene fragment (in terms of the AM theory) are also presented in Table 1. According to the data obtained, the Bpe molecules participate

indeed in the formation of $\pi-\pi$ interactions due to the carbon atoms of the ethylene fragments and heterocycles. The formation of four-membered rings as a combination of two covalent (generalized in terms of the AM theory) and two intermolecular (interactions of closed shells) contacts involving the carbon atoms of the ethylene fragment was observed in none of two compounds. Instead this, seven- and five-membered rings are formed in compounds **I** and **II**, respectively (Fig. 1). It can be assumed that the absence of four-membered rings is caused by either the nonparallel (in compound **I**) or shifted (in compound **II**) arrangement of the Bpe molecules relative to each other, or an insignificant curvature of the electron density above the double bond surface. In addition to the $\pi-\pi$ interactions, an analysis of the electron density revealed hydrogen bonds, and contacts $\text{H}\cdots\text{H}$, $\text{N}\cdots\text{O}$, $\text{C}\cdots\text{O}$, and $\text{C}\cdots\text{H}$. All intermolecular interactions are characterized by $\nabla^2\rho(\mathbf{r}) > 0$ and $h_e(\mathbf{r}) > 0$ at the points $(3, -1)$, which makes it possible to assign them to interactions of closed shells.

Thus, we showed for the first time the bonding routes and the common intermolecular surface between the photosensitive 1,2-bis(4-pyridine)ethylene fragments in the coordination compounds of zinc. This result means that both methods can be applied to other potentially photosensitive compounds for predicting their reactivity in [2+2] photoaddition and makes it possible to considerably facilitate the search for compounds in which solid-phase reactions can occur and to extend the range of types of photoreactions involving coordination compounds.

Table 1. Topological characteristics of coordination bonds and $\pi-\pi$ interactions in the structures of compounds **I** and **II***

Bond	Distance, Å	$\rho(\mathbf{r})$, e Å ⁻³	$\nabla^2\rho(\mathbf{r})$, e Å ⁻⁵	$V_e(\mathbf{r})$, au	$h_e(\mathbf{r})$, au	E_b , kcal/mol
I						
Zn(1)–N(1)	2.032	0.40	14.6	0.103	0.127	32.26
Zn(1)–N(2)	2.042	0.39	13.9	0.097	0.120	30.34
Zn(1)–O(1)	1.994	0.35	11.0	0.083	0.097	26.09
Zn(1)–O(4)	2.015	0.37	10.7	0.080	0.097	25.19
C(6)…C(9a)	3.586	0.05	0.52	0.004	0.0045	1.10
C(7)…C(3b)	3.862	0.04	0.40	0.003	0.0033	0.79
II						
Zn–N(1)	2.158	0.43	1.77	0.066	0.042	20.58
Zn(1)–O(1)	2.160	0.38	2.70	0.056	0.042	17.61
Zn(1)–O(1c)	2.148	0.38	2.70	0.058	0.043	18.18
C(5)…C(5d)	3.524	0.03	0.32	0.002	0.003	0.55
C(4)…C(9d)	3.417	0.03	0.37	0.002	0.003	0.66

* $\rho(\mathbf{r})$ is the electron density at the critical point $(3, -1)$, $\nabla^2\rho(\mathbf{r})$ is the corresponding Laplacian of the electron density, $V_e(\mathbf{r})$ is the potential energy density, $h_e(\mathbf{r})$ is the local electron energy density, and E_b is the interaction energy estimated by the Espinosa–Molins–Lecomte equation [32]: $E_b = -1/2 V_e(\mathbf{r})$. Symmetry codes: (a) $-x - 1, y + 3/2, -z + 3/2$; (b) $-x - 2, y + 3/2, -z + 3/2$; (c) $-x, -y + 1, -z$; (d) $-x + 1/2, y + 1/2, -z$.

ACKNOWLEDGMENTS

The DFT calculations and crystal chemical analysis were supported by the Russian Science Foundation (project no. 17-13-01442). The synthesis of the compounds was supported by the Russian Foundation for Basic Research (project no. 16-33-60179). A.A. Korlyukov is grateful to the Samara Center for Theoretical Materials Science (Samara, Russian Federation) for presented computational sources.

REFERENCES

1. Vittal, J.J., *Coord. Chem. Rev.*, 2007, vol. 251, nos. 13–14, p. 1781.
2. Vittal, J.J. and Quah, H.S., *Coord. Chem. Rev.*, 2017, vol. 342, p. 1.
3. Huang, S.-L., Hor, T.S.A., and Jin, G.-X., *Coord. Chem. Rev.*, 2017, vol. 346, p. 112.
4. Cohen, M.D., *Angew. Chem., Int. Ed. Engl.*, 1975, vol. 14, no. 6, p. 386.
5. Kaupp, G., *Angew. Chem., Int. Ed. Engl.*, 1992, vol. 31, no. 5, p. 595.
6. Mir, M.H., Koh, L.L., Tan, G.K., and Vittal, J.J., *Angew. Chem., Int. Ed. Engl.*, 2010, vol. 49, no. 2, p. 390.
7. Liu, D., Ren, Z.-G., Li, H.-X., et al., *Angew. Chem., Int. Ed. Engl.*, 2010, vol. 49, no. 28, p. 4767.
8. Michaelides, A., Skoulika, S., and Siskos, M.G., *Chem. Commun.*, 2011, vol. 47, no. 25, p. 7140.
9. Li, G.-L., Liu, G.-Z., Ma, L.-F., et al., *Chem. Commun.*, 2014, vol. 50, no. 20, p. 2615.
10. Bogadi, R.S., Levendis, D.C., and Coville, N.J., *J. Am. Chem. Soc.*, 2002, vol. 124, no. 6, p. 1104.
11. Zheng, S.-L., Vande Velde, C.M.L., Messerschmidt, M., et al., *Chem.-Eur. J.*, 2008, vol. 14, no. 2, p. 706.
12. Collet, E., Lorenc, M., Cammarata, M., et al., *Chem.-Eur. J.*, 2012, vol. 18, no. 7, p. 2051.
13. Das, A., Reibenspies, J.H., Chen, Y.-S., and Powers, D.C., *J. Am. Chem. Soc.*, 2017, vol. 139, no. 8, p. 2912.
14. Avdeeva, V.V., Buzin, M.I., Dmitrienko, A.O., et al., *Chem.-Eur. J.*, 2017, vol. 23, no. 66, p. 16819.
15. Gnanaguru, K., Ramasubbu, N., Venkatesan, K., and Ramamurthy, V., *Org. Chem.*, 1985, vol. 50, no. 13, p. 2337.
16. Ushakov, E.N., Vedernikov, A.I., Lobova, N.A., et al., *J. Phys. Chem. A*, 2015, vol. 119, no. 52, p. 13025.
17. Bader, R.F.W., *Atoms in Molecules, A Quantum Theory*, Oxford: Oxford Univ., 1990.
18. Blatov, V.A. and Serezhkin, V.N., *Rus. J. Inorg. Chem.*, 2000, vol. 45, suppl. 2, p. 2.
19. Zorina-Tikhonova, E.N., Chistyakov, A.S., Kis-kin, M.A., et al., *IUCRJ*, 2018, vol. 5, no. 3, p. 293.
20. Kresse, G. and Hafner, J., *Phys. Rev. B*, 1993, vol. 47, no. 1, p. 558.
21. Kresse, G. and Furthmüller, J., *Phys. Rev. B*, 1996, vol. 54, no. 16, p. 11169.
22. Kresse, G. and Furthmüller, J., *Comput. Mater. Sci.*, 1996, vol. 6, no. 6, p. 15.
23. Grimme, S., Ehrlich, S., and Goerigk, L., *J. Comput. Chem.*, 2011, vol. 32, no. 7, p. 1456.
24. Otero-de-la-Roza, A., Johnson, E.R., and Luana, V., *Comput. Phys. Commun.*, 2014, vol. 185, no. 3, p. 1007.
25. Blatov, V.A., Shevchenko, A.P., and Proserpio, D.M., *Cryst. Growth Des.*, 2014, vol. 14, no. 7, p. 3576.
26. Blatova, O.A., Blatov, V.A., and Serezhkin, V.N., *Acta Crystallogr. Sect. B: Struct. Sci.*, 2001, vol. 57, no. 2, p. 261.
27. Peresypkina, E.V. and Blatov, V.A., *Acta Crystallogr. Sect. B: Struct. Sci.*, 2000, vol. 56, no. 6, p. 1035.
28. Serezhkin, V.N. and Savchenkov, A.V., *Cryst. Growth Des.*, 2015, vol. 15, no. 6, p. 2878.
29. Vologzhanina, A.V. and Lyssenko, K.A., *Russ. Chem. Bull.*, 2013, vol. 62, no. 8, p. 1786.
30. Smol'yakov, A.F., Korlyukov, A.A., Dolgushin, F.M., et al., *Eur. J. Inorg. Chem.*, 2015, vol. 2015, no. 36, p. 5847.
31. Carugo, O., Blatova, O.A., Medrish, E.O., et al., *Sci. Rep.*, 2017, vol. 7, p. 13209.
32. Espinosa, E., Molins, E., and Lecomte, C., *Chem. Phys. Lett.*, 1998, vol. 285, nos. 3–4, p. 170.

Translated by E. Yablonskaya